Circular polarization in pulsar integrated profiles

J. L. Han,[1] R. N. Manchester,[2] R. X. Xu[3] and G. J. Qiao[3,4,5]

[1]*Beijing Astronomical Observatory, Chinese Academy of Sciences (CAS), Beijing 100012, China*
[2]*Australia Telescope National Facility, CSIRO, PO Box 76, Epping, NSW 2121, Australia*
[3]*Department of Geophysics, Peking University (PKU), Beijing 100871, China*
[4]*CCAT (World Laboratory), PO Box 8730, Beijing 100080, China*
[5]*Beijing Astrophysical Center, CAS-PKU, Beijing 100871, China*

ABSTRACT

We present a systematic study of the circular polarization in pulsar integrated profiles, based on published polarization data. For core components, we find no significant correlation between the sense change of circular polarization and the sense of linear position-angle variation. Circular polarization is not restricted to core components and, in some cases, reversals of circular polarization sense are observed across the conal emission. In conal double profiles, the sense of circular polarization is found to be correlated with the sense of position-angle variation. Pulsars with a high degree of linear polarization often have one hand of circular polarization across the whole profile. For most pulsars, the sign of circular polarization is the same at 50-cm and 20-cm wavelengths, and the degree of polarization is similar, albeit with a wide scatter. However, at least two cases of frequency-dependent sign reversals are known. This diverse behaviour may require more than one mechanism to generate circular polarization.

Key words: polarization – surveys – pulsars: general.

1 INTRODUCTION

From the earliest observations (e.g. Clark & Smith 1969), it has been clear that individual pulses from pulsars have high linear and circular polarization, often with a sense change of circular polarization through the pulse. The polarization distribution diagrams of Manchester, Taylor & Huguenin (1975), Backer & Rankin (1980) and Stinebring et al. (1984a,b) show clearly the variable nature of the circular polarization. Very high degrees of circular polarization are occasionally observed in individual pulses, even up to 100 per cent (Cognard et al. 1996) and mean values are typically 20–30 per cent.

Integrated or average pulse profiles generally have a much smaller degree of circular polarization (e.g. Lyne, Smith & Graham 1971; Manchester 1971), showing that the sign of the circular Stokes parameter V (here defined to be $I_{LH} - I_{RH}$) is variable at a given pulse phase. Significant net V is observed in the mean pulse profiles of most pulsars. In many cases, it is concentrated in the central part of the profile and shows a reversal of sense near the centre, but in other pulsars the same sense is retained throughout. It is common to identify a central peak or region of a profile as 'core' emission, and the outer parts as 'conal' emission (Rankin 1983; Lyne & Manchester 1988). Various properties, for example, spectral index, often vary from the central to the outer parts of a profile. Rankin (1983) suggested that core and conal emissions have different emission mechanisms, with circular polarization being a property of core emission only, but Lyne & Manchester (1988) and Manchester (1995) argued that there is

merely a gradation of properties across the whole emission beam. Radhakrishnan & Rankin (1990) identified two types of circular polarization: 'antisymmetric', in which there is a sense change near the centre of the profile, and 'symmetric', where the same hand of circular polarization is observed across the pulse profile. In pulsars with antisymmetric V, they found a correlation of the direction of circular sense change with the direction of linear position-angle (PA) swing.

The observed diverse circular polarization properties may relate to the the pulsar emission mechanism or to propagation effects occurring in the pulsar magnetosphere (cf. Melrose 1995). In the widely adopted magnetic pole models (Radhakrishnan & Cooke 1969; Komesaroff 1970; Sturrock 1971; Ruderman & Sutherland 1975), it seems very difficult to explain various circular polarization behaviours. Cheng & Ruderman (1979) suggested that the expected asymmetry between the positively and negatively charged components of the magnetoactive plasma in the far magnetosphere of pulsars will convert linear polarization to circular polarization. On the other hand, Kazbegi, Machabeli & Melikidze (1991, 1992) argued that the cyclotron instability, rather than the propagation effect, is responsible for the circular polarization of pulsars. Other authors have argued for its intrinsic origin (Michel 1987; Gil & Snakowski 1990a,b; Radhakrishnan & Rankin 1990; Gangadhara 1997). In summary, the observed circular polarization of pulsar radiation is presently not well understood.

This paper attempts to summarize the main features of the observed circular polarization in pulsar mean pulse profiles and to
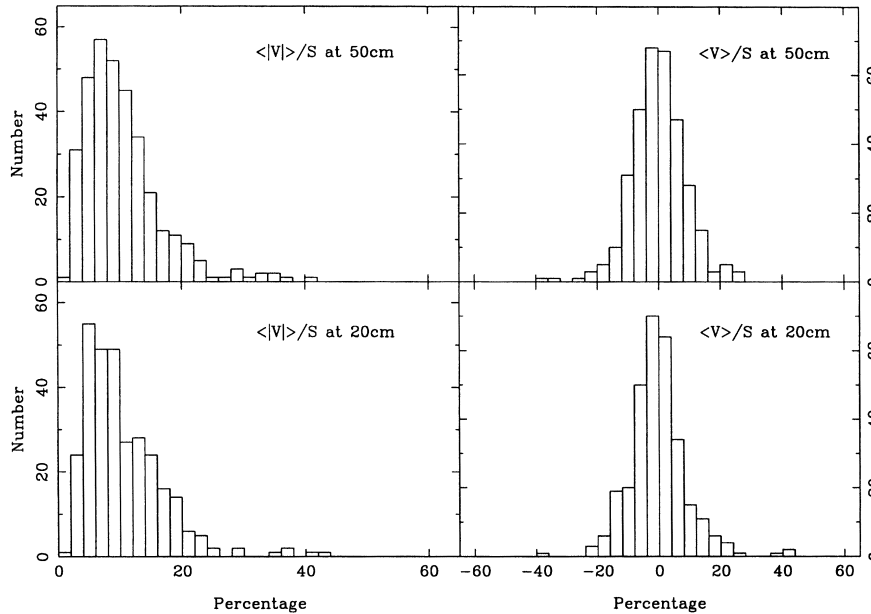
Figure 1. Distribution of $\langle|V|\rangle/S$ and $\langle V\rangle/S$ at wavelengths of 50 cm and 20 cm.

discuss these in the context of other pulsar properties. We outline the main characteristics of pulsar circular polarization in Section 2, discuss possible mechanisms for the generation of circular polarization in Section 3, and present our conclusions in Section 4.

2   CIRCULAR POLARIZATION PROPERTIES

Information about circular polarization and PA variations from all available published polarization profiles is summarized in Appendix A, Table A1. Only pulsars (PSRs) with significant circular polarization (i.e. signal-to-noise ratio in V greater than 3) are included in the table. For about 40 per cent of the pulsars examined, circular polarization is below this threshold. In the following subsections, we discuss various characteristics of the observed circular polarization.

2.1   Degree of circular polarization

Fig. 1 shows histograms of $\langle|V|\rangle/S$ and $\langle V\rangle/S$ in the 50-cm band ($\sim$650 MHz) and 20-cm band ($\sim$1400 MHz), where $S = \langle I\rangle$ is the mean flux density, for the pulsars in Table A1. Levels of circular polarization are very similar at the two wavelengths; the median value of $\langle|V|\rangle/S$ is 9 per cent at 50 cm and 8 per cent at 20 cm. Only a few pulsars have mean circular polarization exceeding 20 per cent. The apparent deficit of pulsars with $\langle|V|\rangle/S \lesssim 5$ per cent is not real; for low signal-to-noise ratio observations, noise in the profile makes a positive contribution to $\langle|V|\rangle/S$. Although the least significant signal-to-noise ratios in V were not included in the sample, many of the profiles have relatively low signal-to-noise ratio and hence a biased estimate of $\langle|V|\rangle/S$.

As Fig. 1 shows, strong circular polarization has been detected from only a small number of pulsars; an example of such a pulsar is shown in Fig. 2. Pulsars with $\langle|V|\rangle/S > 20$ per cent and polarization error < 5 per cent are listed in Table 1. PSR B1702$-$19, an interpulse pulsar, has the highest known fractional circular polarization, up to 60 per cent (Biggs et al. 1988); note, however, that Gould (1994) gives values of 30–35 per cent. PSR B1914+13, a pulsar with almost the same P and $\dot{P}$, and hence the same estimates

of characteristic age, surface magnetic field and total energy-loss rate $\dot{E}$ as PSR B1702$-$19, also has very strong circular polarization (Fig. 2).

As Table 1 shows, all but one of the pulsars with strong circular polarization are symmetric, i.e. with no reversals of V across the pulse profile. These pulsars are discussed further in Section 2.4 below. Although most of these pulsars also have relatively high levels of fractional linear polarization, a few do not.

2.2   Antisymmetric circular polarization and core emission

As mentioned in Section 1, circular polarization is often stronger in the central or core regions of a profile, and often shows a reversal in
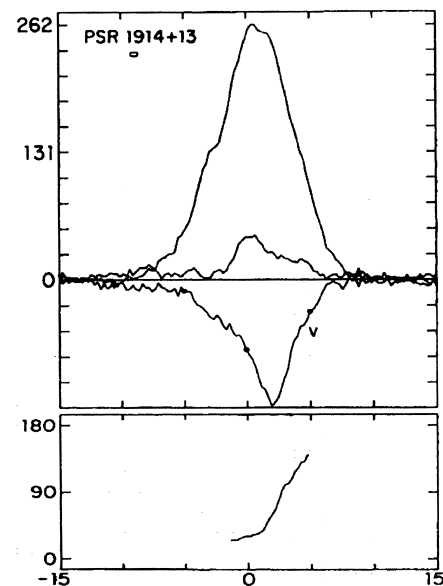

Figure 2. Polarization profile for PSR B1914+13, a pulsar with strong circular polarization over the whole observed profile (from Rankin, Stinebring & Weisberg 1989).

Table 1. Pulsars with strong circular polarization.

PSR	Freq. (MHz)	$\langle|V|\rangle/S$ (%)	$\langle V\rangle/S$ (%)	$\langle L\rangle/S$ (%)	Err. (%)	Ref.
B1702−19	408	60	−60	35	2	B88
B1913+10	1400	38	38	35	2	R89
B1914+13	1400	37	−37	18	2	R89
B0835−41	405	35	35	3	3	H77
B1221−63	950	33	26	30	5	Mc78, V97
B1557−50	1612	23	21	11	4	Ma80
B0942−13	408	23	19	22	1	G94
J1359−6038	660	22	22	83	2	M98
B2327−20	648	22	−22	16	1	Mc78
B1737−30	1560	22	−22	87	3	W93
B1952+29	1400	21	−19	18	1	R89
B1857−26	1612	20	−1	23	3	Ma80

References: Hamilton et al. 1977 (H77); McCulloch et al. 1978 (Mc78); Manchester, Hamilton & McCulloch 1980 (Ma80); Biggs et al. 1988 (B88); Rankin, Stinebring & Weisberg 1989 (R89); Wu et al. 1993 (W93); Gould 1994 (G94); van Ommen et al. 1997 (V97); Manchester, Han & Qiao 1998 (M98).

sign near the profile centre. From a sample of 25 pulsars, Radhakrishnan & Rankin (1990) found a correlation between the sense of the sign reversal and the sense of PA swing, with transitions of circular polarization from left-handed LH to right-handed RH (+/−) being associated with decreasing PA (clockwise rotation on the sky) across the profile, and vice versa. The proposed correlation was questioned by Gould (1992, 1994) who found some contrary examples.

Table 2 lists pulsars with a reversal in the sign of V in the central or core region of the profile, and two good examples are shown in Fig. 3. In Table 2, pulsars are divided into different columns according to the sense of the V sign change and the direction of PA swing. Further information about the observations can be found in Table A1. Among 27 pulsars listed, 12 pulsars (in the first and fourth columns) agree with the correlation proposed by Radhakrishnan & Rankin (1990) and 15 pulsars (in the second and third columns) disagree. We therefore conclude that there is no correlation between the sense of the sign change of circular polarization and the sense of variation of linear polarization angle across the profile. Consequently, theoretical discussions based on this correlation (e.g. Radhakrishnan & Rankin 1990; Kazbegi et al. 1991) are not well founded.

It is worth noting that central or 'core' reversals in circular polarization sense usually occur very close to the mid-point of the

Table 2. Circular sign reversals and sign of PA variation.

LH/RH = +/−		RH/LH = −/+	
PA: dec	PA: inc	PA: dec	PA: inc
B1237+25	B0823+26m	B0329+54	B0450−18
B1508+55	J1001−5507?[a]	J0437−4715	B1700−32
B1737+13	J1604−4909	B0942−13	J2144−3933
J1801−0357?[a]	B2002+31	B1323−58	
B1821+05?[a]	B2003−08	B1451−68	
B1857−26	B2113+14	J1527−5552	
B1859+03		B1534+12	
B2045−16		J1852−2610	
B2111+46		B1907+02	

[a]For PSRs B1821+05, J1801−0357 and J1001−5507, the PA variation is not very clear.
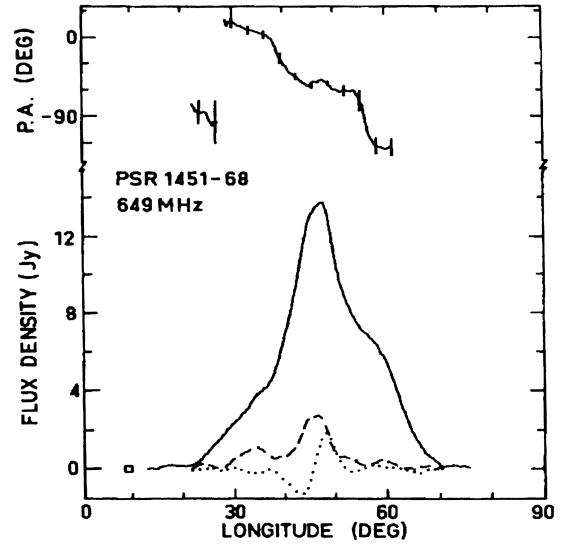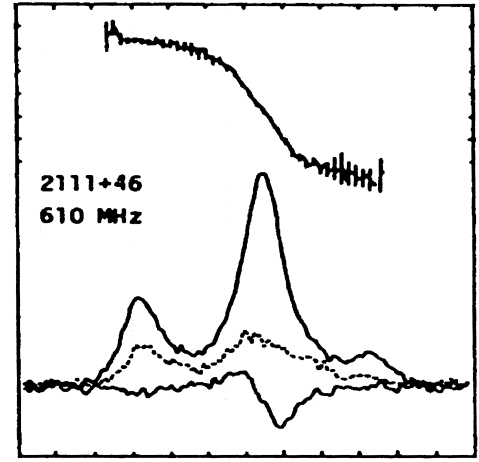
Figure 3. Two examples of pulsars with central reversals in the sign of V (from Lyne & Manchester 1988; McCulloch et al. 1978).

pulse profile and do not appear to be related to any particular peak in the total intensity profile. For example, PSR B0149−16 at 50 cm (Qiao et al. 1995) has a central reversal in V between two overlapping pulse components; PSRs B1855+09 (main pulse) and B1933+16 (Segelstein et al. 1986; Rankin et al. 1989) are similar. In other pulsars, e.g. PSRs B1451−68 and B2003−08, the central peak is offset in longitude from the profile mid-point. Some conal double pulsars, such as PSR B2048−72, have a clear central reversal but no core component at all. These observations suggest that the 'core' sense reversal is associated with the central region of the beam, rather than with any particular component.

2.3 Circular polarization in cone-dominated pulsars

It is often stated that the conal components of pulsar profiles have weak or no circular polarization (e.g. Radhakrishnan & Rankin 1990; Gil et al. 1995). However, there are many examples of significant circular polarization in profiles, or parts of profiles, which are believed to be conal emission. Fig. 4 shows two 'conal-double' pulsars which show significant circular polarization.

In most cases, the circular polarization is symmetric, i.e. it has the same sign over the profile. In Table 3, we show the relationship between the sign of PA variation and sense of circular polarization
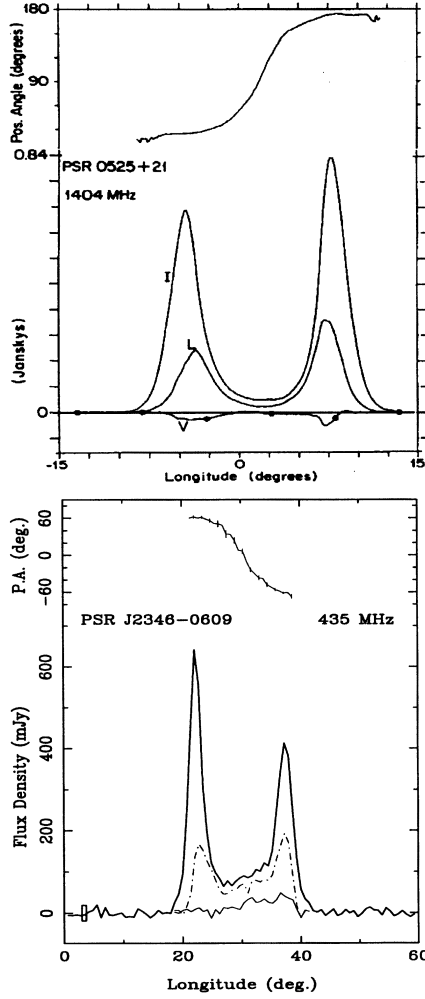
Figure 4. Two examples of conal-double pulsars with significant circular polarization (from Stinebring et al. 1984a; Manchester, Han & Qiao 1998).

Table 3. Conal-double pulsars with significant circular polarization.

PSR	PA	Sign of V		Ref.
		Comp 1	Comp 2	
B0148−06	inc	−	−	LM88
B0525+21	inc	−	−	S84a, R83
B0751+32	inc	−	−	R89
B0818−13	inc	−	−	V97, Q95, B87
B0834+06	inc	−	−	Mc78, S84a
		+/−	−	S84b
B1133+16	inc	−	−	Mc78, S84a
B1913+16	inc	−/+	−	C90
B2020+28	inc	+/−	−	C78, S84a
B2044+15	inc	−	−	G94
B2048−72	inc	±	∓	Q95, M98
B0301+19	dec	+	+	R83, R89
J0631+1036	dec	+	+	Z96
B1039−19	dec	−/+	+	LM88, G94
J1123−4844	dec	+	+	M98
B1259−63	dec	+	·	MJ95
J1527−3931	dec	+	+	M98
B1727−47	dec	+	·	H77, Mc78, V97
J1751−4657	dec	−/+	+	M98
B2321−61	dec	+	·	Q95
J2346−0609	dec	·	+	M98

References: Hamilton et al. 1977 (H77); Cordes, Rankin & Backer 1978 (C78); McCulloch et al. 1978 (Mc78); Rankin 1983 (R83); Stinebring et al. 1984a (S84a); Stinebring et al. 1984b (S84b); Biggs et al. 1987 (B87); Lyne & Manchester 1988 (LM88); Rankin, Stinebring & Weisberg 1989 (R89); Cordes, Wasserman & Blaskiewicz 1990 (C90); Gould 1994 (G94); Manchester & Johnston 1995 (MJ95); Qiao et al. 1995 (Q95); Zepka, Cordes & Wasserman 1996 (Z96); van Ommen et al. 1997 (V97); Manchester, Han & Qiao 1998 (M98).

in conal-double pulsars. A striking conclusion is that there is a strong correlation between these two properties, with right-hand (negative) circular polarization accompanying increasing PA and vice versa. No good examples contrary to this trend have been found. Therefore, unlike the correlation between the sense of sign change in core emission and PA swing, this correlation appears to be significant.

In some cases, a change in the sign of V is observed, generally associated with the first component. Exceptions are PSR B2048−72, where it is centrally located, and PSR B0329+54 in its 'abnormal' mode, where there is a sense change in the trailing conal component (Xilouris et al. 1995). Note also that, for PSR B0834+06, there is a sign change under the first component at 800 MHz, but not at 1404 MHz (Stinebring et al. 1984a,b).

In summary, these observations show that circular polarization and sense changes are not associated with any particular 'core' component. The implication is that there is no fundamental difference between core and conal emission.

2.4 Symmetric circular polarization

For a number of pulsars, we see one hand of circular polarization over the whole profile, the so-called 'symmetric' type by Radhakrishnan & Rankin (1990). Table 4 lists pulsars of this type; see Table

A1 for more observation details and references. Most of these pulsars have one component or several unresolved components, and a large majority have strong linear polarization. A good example, PSR B0628−28, is shown in Fig. 5.

It is worth mentioning that receiver cross-coupling can result in spurious circular polarization in strongly linearly polarized sources (e.g. Rankin & Benson 1981; Thorsett & Stinebring 1990). However, we believe that this is not relevant for most of the pulsars listed here, and hence that the correlation of symmetric circular polarization with strong linear polarization is real.

The emission from these pulsars is probably conal, either from a grazing cut of the emission beam (as in PSR B0628−28), or from a

Table 4. Pulsars with symmetric circular polarization.

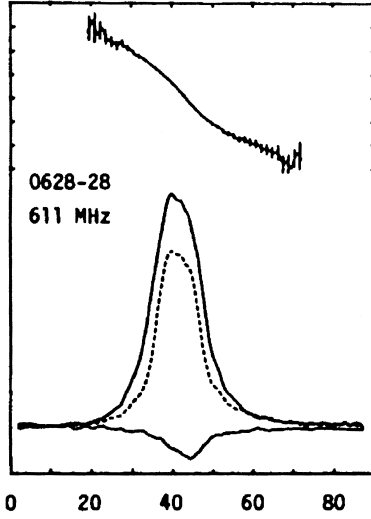| LH = +		RH = −	
PA: inc	PA: dec	PA: inc	PA: dec
B0611+22	B1913+10?	J0134−2937	B0538−75?
B0835−41		J1603−5657	B0540+23
J0942−5657		B1706−14	B0628−28
J1202−5820		B1914+13	B0740−28
J1253−5820		B2315+21	B0833−45
J1359−6038		B2327−20	B0950+08
J1722−3712			B1629−50?
			B1702−19m
			B1702−19i
			B1737−30
			B1915+13
			B1937−26

Figure 5. PSR B0628−28, an example of a pulsar with 'symmetric' circular polarization and high linear polarization (from Lyne & Manchester 1988).

leading or trailing component. Many of these pulsars are in the young and highly polarized class identified by Manchester (1996) as having very wide conal beams. As shown above, conal-double pulsars, for which the emission comes from beam edge, generally have a single sense of circular polarization over each component. However, Table 4 shows that the correlation between sign of V and sense of PA swing observed in conal-double pulsars is not seen in the symmetric-V pulsars.

2.5 Complex variations of circular polarization with longitude

As described above, circular polarization from central or core regions of the profile is usually antisymmetric, whereas that from conal regions is usually symmetric. In some pulsars, e.g. PSR B2003−08 (Fig. 6) these two properties are superimposed, result-ing in a more complex pattern of V sign changes across the profile.

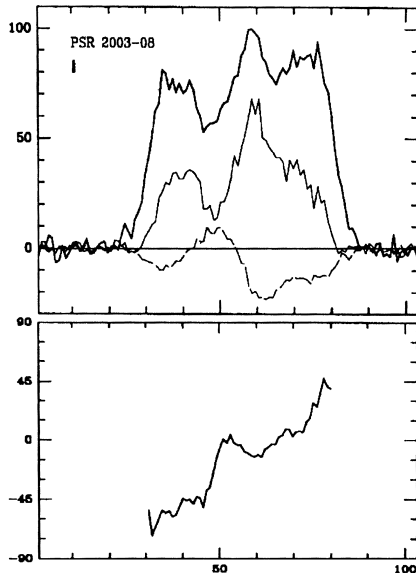Complex variations, possibly related to different components of

Figure 6. PSR B2003−08, a pulsar showing both symmetric and antisym-metric circular polarization (from Xilouris et al. 1991).
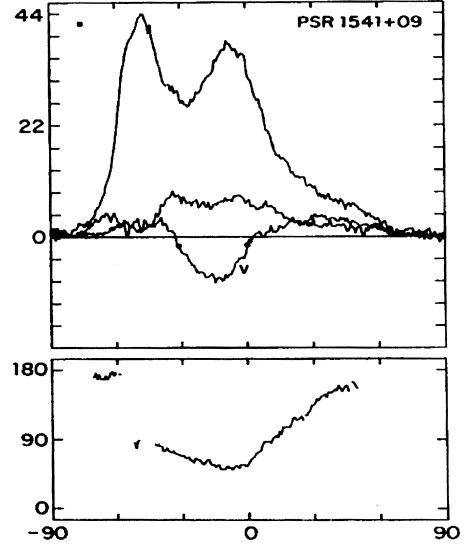
Figure 7. PSR B1541+09, a pulsar with a complex variation of circular polarization across the profile (from Rankin et al. 1989).

the profile, are seen in PSR B1541+09 (Fig. 7) and PSR B1952+29 (Rankin et al. 1989). PSR B1907+10 (Rankin et al. 1989) has relatively strong RH circular polarization, apparently related to one component of the profile.

Without doubt, the most complex variation of circular (and linear) polarization known is seen in PSR J0437−4715 (Navarro et al. 1997). As with many other pulsars, circular polarization is strongest near the main central peak of the profile and has a sign reversal at or near the profile centre. However, circular polarization is detected over most of the very wide pulse profile, with several sense reversals at other longitudes. On the leading side of the profile, these reversals may be centred on pulse components, but this is not the case on the trailing side.

2.6 Frequency dependence of circular polarization

As discussed in Section 2.1, there is little systematic difference in the degree of circular polarization between frequencies of 650 MHz (50 cm) and 1400 MHz (20 cm). This is further illustrated in Fig. 8, which shows the distributions of ratios of $\langle|V|\rangle/S$ and $\langle V\rangle/S$ at 50 and 20 cm. In both cases, the distributions are centred on 1.0 (in fact, the median value of $[\langle|V|\rangle/S]_{50}/[\langle|V|\rangle/S]_{20}$ is exactly 1.0), showing that there is little or no systematic variation in degree of circular polarization with frequency.

However, these histograms do have a wide spread. A significant number of $[\langle V\rangle/S]_{50}/[\langle V\rangle/S]_{20}$ values are negative, implying a change in sign of $\langle V\rangle$ with frequency. Fig. 9 shows the frequency dependence of $\langle V\rangle/S$ in more detail for three pulsars. For two of these, there is clear evidence for a change in sign of $\langle V\rangle$.

Table 5 lists pulsars with apparently significant frequency-dependent circular polarization. In some cases, such as those shown in Fig. 9, there seems no doubt about the reality of the frequency dependence. In other cases, further observations are required to establish these trends with more certainty. Simultaneous dual-frequency observations would be especially interesting.

3 DISCUSSION

We have presented a summary of all published observations relating to circular polarization of pulsar mean pulse profiles. We emphasize
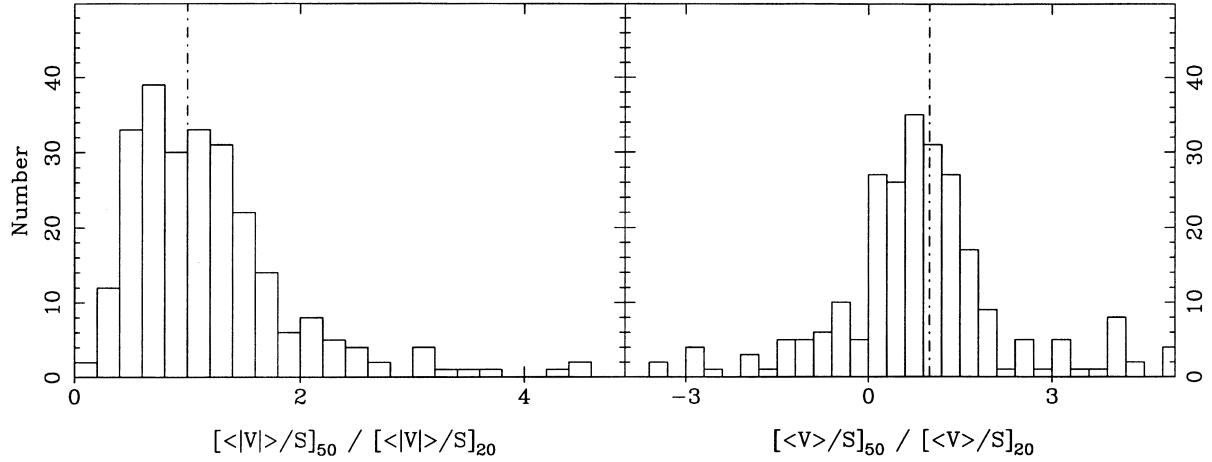
Figure 8. Distribution of ratios of $\langle|V|\rangle/S$ and $\langle V\rangle/S$ at wavelengths of 50 cm and 20 cm. The dot-dashed line marks a ratio of 1.0.

that we have not considered polarization of individual pulses. While individual pulse polarization may be closely related to the generation process, published results are not as complete and the properties are very variable, making analysis difficult. In general, characteristics of the mean pulse profile are stable in time, and hence provide a framework for understanding the processes related to generating the polarization.

Generally, in astronomy, wherever there is appreciable asymmetry, there is likely to be polarization at some level (Tinbergen 1996, p.27). If the asymmetry is of a scalar kind (e.g. a longitudinal component of the magnetic field), the polarization or birefringence will be circular and scalar in character. If the asymmetry is of a vector type (e.g. a transverse magnetic component), the polarization or birefringence will be linear and vector in character.

For pulsars, the radio emission is believed to be generated by highly relativistic particles moving along magnetic field lines above the magnetic poles. These field lines are curved, giving the asymmetry a vector component which, from the general principle

above, results in linear polarization as in the widely accepted rotating-vector model (Radhakrishnan & Cooke 1969). There are strong curved magnetic fields, not only in the emission region, but also along the path in the pulsar magnetosphere through which the radiation propagates. The emission region is very probably asymmetric and the emission beam is anisotropic. Hence, the observed circular polarization can be either intrinsic to the emission process or caused by propagation effects, or perhaps both.

3.1 Intrinsic origin?

If the observed circular polarization is intrinsic to the emission region or radiation process, the radiation should suffer negligible modification by propagation effects. With one or two possible exceptions, the sense reversal of circular polarization seen in central

Table 5. Pulsars showing frequency-dependent circular polarization.

PSR	low ν	high ν	Ref.
B0148−06	−	none?	LM88, W93
B0149−16	+−	none?	Q95, X91
B0355+54	weak	strong	LM88, X91, X95
B0833−45	weak	strong	H77, Ma80, KD83
B0834+06	+/ − −	− + −	S84ab, V97, Ma80
B0835−41	strong	weak	H77, Mc78, Ma80
B0932−52	−	+?	V97, M98
B1240−64	+	−	Mc78, V97, Ma80
B1641−68	strong	none?	Q95, V97, W93
B1700−32	none?	−/+	LM88, Ma80
B1727−47	weak	none?	H77, Mc78, V97, Ma80
B1749−28	−	−/+	Mc78, V97, Ma80, Mr81
B2048−72	+/−	−/+	Q95

References: Hamilton et al. 1977 (H77); McCulloch et al. 1978 (Mc78); Manchester, Hamilton & McCulloch 1980 (Ma80); Morris et al. 1981 (Mr81); Krishnamohan & Downs 1983 (KD83); Stinebring et al. 1984a (S84a); Stinebring et al. 1984b (S84b); Lyne & Manchester 1988 (LM88); Xilouris et al. 1991 (X91); Wu et al. 1993 (W93); Qiao et al. 1995 (Q95); Xilouris et al. 1995 (X95); van Ommen et al. 1997 (V97); Manchester, Han & Qiao 1998 (M98).
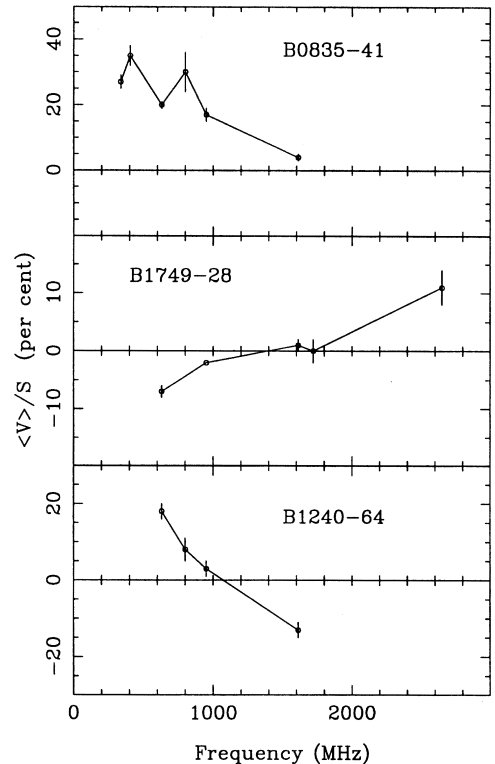

Figure 9. Frequency dependence of $\langle V\rangle/S$ for three pulsars.

or core regions of pulsar profiles is not frequency-dependent, which suggests that the circular polarization does not arise from a propagation effect or plasma emission process (Michel 1987; Radhakrishnan & Rankin 1990). An origin related to asymmetry in the beam shape seems more likely.

If the extent of the radio emission beam is determined by the last open magnetic field lines from the polar cap, it is axisymmetric for an aligned rotator. However, the axisymmetry is broken for oblique rotators. For purely geometric reasons, the beam is elongated in the longitude direction (Biggs 1990; Roberts & Sturrock 1972).

Michel (1987) suggested that the currents out of a polar cap should preferentially flow along the shortest open field lines to the light cylinder and argued that pulsar radiation is not from a complete hollow cone, but is concentrated in the half-cone at lower latitude. In contrast, in the model developed by Arons and co-workers (e.g. Arons 1983), relativistic charged particles accelerate within the flux tubes of 'favourable curvature' which bend towards the rotation axis. Pulsar emission then is only possible from the upper half-beam at high latitudes.

If the pulsar radio beam is randomly patchy in structure as suggested by Lyne & Manchester (1988) and emission is generated by relativistic particles flowing along random flux tubes, then other asymmetries will be present. The fact that multiple and asymmetric components are observed in pulse profiles shows that such asymmetries exist. These may, for example, account for the complex longitude variation of pulsar circular polarization seen in pulsars such as PSR J0437−4715.

Radhakrishnan & Rankin (1990) suggested that the elliptical shape of the pulsar beam is responsible for the antisymmetric polarization for core components. According to this model, the circular polarization should be intrinsically antisymmetric and frequency-independent. Radhakrishnan & Rankin (1990) argued that this mechanism could produce the correlation between sense change and PA variation. However, as discussed in Section 2.2, this correlation is no longer observed, indicating a different origin for the circularly polarized emission.

Gangadhara (1997) has suggested that positrons and electrons emit orthogonally polarized emission as they move along curved magnetic field lines. If the trajectories of the two species are different, coherent superposition of the two orthogonal modes would result in antisymmetric circular polarization.

3.2 Propagation effect or plasma process?

In a relativistic electron–positron plasma, for $\theta \ll 1$, $\omega_p^2/\omega_B^2 \ll 1$ and $\Delta\gamma/\gamma_p \ll 1$, two circularly polarized waves can exist if

$$\theta^2 \ll \theta_0^2 \equiv (\omega/8\omega_B)(\Delta\gamma/\gamma_p^4),$$

and two linear polarization waves can exist in the opposite case, i.e. $\theta^2 \gg \theta_0^2$ (Shafranov 1967; Kazbegi et al. 1991, 1992). Here, $\omega_B = eB/mc$, $\omega_p^2 = 4\pi ne^2/m$, θ is the angle between the wavevector and the local magnetic field direction, and γ_p is the average Lorentz factor of the plasma. The average difference, $\Delta\gamma$, of Lorentz factors for $e^\pm$ plays a critical role in the polarization properties. If $\Delta\gamma$ is very small so that $\theta^2 \gg \theta_0^2$ is always satisfied, then we have only linear polarization modes. Conversely, when the distributions of electrons and positrons are significantly different, circular polarization waves can exist and propagate in the region of $\theta^2 \ll \theta_0^2$. This concurs with the simple principle that circular polarization is related to the longitudinal magnetic field, and allows circular polarization to propagate near the magnetic axis where the angle between the wavevector and the magnetic field can be always small.

Cheng & Ruderman (1979) introduced the term 'adiabatic walking' to describe the slow change in the polarization properties during propagation in the pulsar magnetosphere. This effect can result in 100 per cent linearly polarized wave modes even when the generated waves have random polarization. In the far magnetosphere, the conditions for adiabatic walking no longer apply, and circularly polarized modes can be generated. Two distinct mechanisms were discussed. One applies to a symmetric $e^\pm$ plasma, i.e. the positrons and electrons have the same distribution of Lorentz factors. Adiabatic walking fails near the light cylinder if the propagation direction and magnetic field are no longer coplanar; the initially linearly polarized modes then become elliptical. The second mechanism is for an asymmetric plasma. The normal modes become elliptical when the inequality $\omega \ll \gamma(eB/mc)$ is no longer satisfied because of diminishing B. Significant circular polarization can be generated before adiabatic walking ceases, so long as the curvature of field lines is sufficiently small. Cheng & Ruderman (1979) believe that this second mechanism is likely to be more significant.

Both mechanisms predict a frequency dependence of circular polarization, with weaker polarization at higher frequencies. As discussed in Section 2.6, this is seen in some pulsars, but is not generally the case. Observations over a wider frequency range would be useful.

The region of cyclotron resonance, typically located several hundred neutron-star radii above the surface, is an interesting region, where

$$|\omega_B|/\gamma = \omega(1 - \beta\cos\theta) \simeq \omega(\theta^2 + \gamma^{-2})/2.$$

Here $\beta = v/c$ for the particles. Kazbegi et al. (1991) suggested that pulsar emission is generated in this region via the cyclotron instability. For large θ, the emission is linearly polarized, but for small θ it is circularly polarized with sense corresponding to the charge signs. Net circular polarization can be produced by a relativistic electron–positron plasma with $\Delta\gamma \neq 0$. This mechanism would be expected to produce circular polarization predominantly in the central or core regions of the profile.

Propagation through this region may alter the polarization state of a wave. Istomin (1992) suggested that incident linearly polarized waves become circular as a result of generalized Faraday rotation in this region. Radiation with a wavevector in the plane of the field line (O mode) becomes LH polarized and that with a wavevector normal to the plane (E mode) becomes RH polarized. The two circular modes have different group velocities, which could result in net circular polarization in the observed radiation. This is a possible origin for 'symmetric' circular polarization observed in conal emission (Table 4).

4 CONCLUSIONS

We have shown that, in pulsars, circular polarization is common but diverse in nature. It is generally strongest in the central or 'core' regions of a profile, but is by no means confined to these regions. The circular polarization often changes sense near the middle of the profile, but sign changes are occasionally observed at other longitudes. Relatively strong circular polarization of one hand is often observed in pulsars that also have high linear polarization. Although examples of both increasing and decreasing degree of circular polarization with frequency, and even changes of sign, are observed, on average there is no systematic frequency dependence of polarization degree. The correlation between circular polarization sense and sense of PA swing for conal-double pulsars is very intriguing.

It seems unlikely that these diverse behaviours can be accounted for by a single mechanism for generation of circular polarization. Both intrinsic emission and propagation effects seem possible. Antisymmetric circular emission could result from asymmetries in the emission beam or from propagation effects in the pulsar magnetosphere. Confirmation of its frequency independence would support an intrinsic process. On the other hand, the strong symmetric polarization observed in conal components is most probably generated by a propagation process.

Further observations of the polarization of both individual and mean pulse profiles will help to clarify many of these issues. In particular, observations over a wide frequency range would be valuable in sorting out the importance of propagation effects.

ACKNOWLEDGMENTS

REFERENCES

Arons J., 1983, ApJ, 266, 215
Arzoumanian Z., Phillips J. A., Taylor J. H., Wolszczan A., 1996, ApJ, 470, 1111 (A96)
Backer D. C., Rankin J. M., 1980, ApJS, 42, 143 (BR80)
Barter N., Morris D., Sieber W., Hankins T., 1982, ApJ, 258, 776 (B82)
Biggs J. D., 1990, MNRAS, 245, 514
Biggs J. D., McCulloch P. M., Hamilton P. A., Manchester R. N., Lyne A. G., 1985, MNRAS, 215, 281 (B85)
Biggs J. D., McCulloch P. M., Hamilton P. A., Manchester R. N., 1987, MNRAS, 228, 119 (B87)
Biggs J. D., Lyne A. G., Hamilton P. A., McCulloch P. M., Manchester R. N., 1988, MNRAS, 235, 255 (B88)
Cheng A. F., Ruderman M. A., 1979, ApJ, 229, 348
Clark R. R., Smith F. G., 1969, Nat, 221, 724
Cognard I., Shrauner J. A., Taylor J. H., Thorsett S. E., 1996, ApJ, 457, L81
Cordes J. M., Rankin J. M., Backer D. C., 1978, ApJ, 223, 961 (C78)
Cordes J. M., Wasserman I., Blaskiewicz M., 1990, ApJ, 349, 546 (C90)
Costa M. E., McCulloch P. M., Hamilton P. A., 1991, MNRAS, 252, 13 (C91)
Fruchter A. S. et al., 1990, ApJ, 351, 642 (F90)
Gangadhara R. T., 1997, A&A, 327 155
Gil J. A., Snakowski J. K., 1990a, A&A, 234, 237
Gil J. A., Snakowski J. K., 1990b, A&A, 234, 269
Gil J. A., Kijak J., Maron O., Sendyk M., 1995, A&A, 301, 177
Gould D. M., 1992, in Hankins T. H., Rankin J. M., Gil J. A., eds, Proc. IAU Coll. 128, The Magnetosphere Structure and Emission Mechanism of Radio Pulsars. Pedagogical Univ. Press, Zielona Góra, p. 384
Gould D. M., 1994, PhD thesis, Univ. Manchester (G94)
Hamilton P. A., McCulloch P. M., Ables J. G., Komesaroff M. M., 1977, MNRAS, 180, 1 (H77)
Istomin Ya. N., 1992, in Hankins T. H., Rankin J. M., Gil J. A., eds, Proc. IAU Coll. 128, The Magnetosphere Structure and Emission Mechanism of Radio Pulsars. Pedagogical Univ. Press, Zielona Góra, p. 375
Kazbegi A. Z., Machabeli G. Z., Melikidze G. J., 1991, MNRAS, 253, 377
Kazbegi A. Z., Machabeli G. Z., Melikidze G. J., 1992, in Hankins T. H., Rankin J. M., Gil J. A., eds, Proc. IAU Coll. 128, The Magnetosphere Structure and Emission Mechanism of Radio Pulsars. Pedagogical Univ. Press, Zielona Góra, p. 373
Komesaroff M. M., 1970, Nat, 225, 612
Krishnamohan S., Downs G. S., 1983, ApJ, 265, 372 (KD83)
Lyne A. G., Manchester R. N., 1988, MNRAS, 234, 477 (LM88)
Lyne A. G., Smith F. G., Graham D. A., 1971, MNRAS, 153, 337
McCulloch P. M., Hamilton P. A., Manchester R. N., Ables J. G., 1978, MNRAS, 183, 645 (Mc78)
Manchester R. N., 1971, ApJS, 23, 283 (M71)
Manchester R. N., 1995, JA&A, 16, 107
Manchester R. N., 1996, in Johnston S., Walker M. A., Bailes M., eds, Proc. IAU Coll. 160, Pulsars: Problems and Progress. Astron. Soc. Pac., San Francisco, p. 193
Manchester R.N., Johnston S., 1995, ApJ, 441, L65 (MJ95)
Manchester R. N., Taylor J. H., Huguenin G. R., 1975, ApJ, 196, 83
Manchester R. N., Hamilton P. A., McCulloch P. M., 1980, MNRAS, 192, 153 (Ma80)
Manchester R. N., Han J. L., Qiao G. J., 1998, MNRAS, 295, 280 (M98)
Melrose D. B., 1995, JA&A, 16, 137
Michel F. C., 1987, ApJ, 322, 822
Morris D., Graham D. A., Sieber W., Bartel N., Thomasson P., 1981, A&AS, 46, 421 (Mr81)
Navarro J., Manchester R. N., Sandhu J. S., Kulkarni S. R., Bailes M., 1997, ApJ, 486, 1019 (N97)
Phillips J. A., 1990, ApJ, 361, L57 (P90)
Qiao G. J., Manchester R. N., Lyne A. G., Gould D. M., 1995, MNRAS, 274, 572 (Q95)
Radhakrishnan V., Cooke D. J., 1969, Astrophys. Lett., 3, 225
Radhakrishnan V., Rankin J. M., 1990, ApJ, 352, 258
Rankin J. M., 1983, ApJ, 274, 333 (R83)
Rankin J. M., Benson J. M., 1981, AJ, 86(3), 418 (RB81)
Rankin J. M., Wolszczan A., Stinebring D. R., 1988, ApJ, 324, 1048 (R88)
Rankin J. M., Stinebring D. R., Weisberg J. M., 1989, ApJ, 346, 869 (R89)
Roberts D. H., Sturrock P. A., 1972, ApJ, 172, 435
Ruderman M. A., Sutherland P. G., 1975, ApJ, 196, 51
Segelstein D. J., Rawley L. A., Stinebring D. R., Fruchter A. S., Taylor J. H., 1986, Nat, 322, 714 (S86)
Seiradakis J. H., Gil J. A., Graham D. A., Jessner A., Kramer M., Malofeev V. M., Sieber W., Wielebinski R., 1995, A&AS, 111, 205 (S95)
Shafranov V. D., 1967, Review of Plasma Physics, Vol. 3. Consultants Bureau, New York
Stinebring D. R., Cordes J. M., Rankin J. M., Weisberg J. M., Boriakoff V., 1984a, ApJS, 55, 247 (S84a)
Stinebring D. R., Cordes J. M., Weisberg J. M., Rankin J. M., Boriakoff V., 1984b, ApJS, 55, 279 (S84b)
Sturrock P. A., 1971, ApJ, 164, 529
Thorsett S. E., Stinebring D. R., 1990, ApJ, 361, 644 (TS90)
Tinbergen J., 1996, Astronomical Polarimetry. Cambridge Univ. Press, Cambridge
van Ommen T. D., D'Alessandro F., Hamilton P. A., McCulloch P. M., 1997, MNRAS, 287, 307 (V97)
Wu X. J., Manchester R. N., Lyne A. G., Qiao G. J., 1993, MNRAS, 261, 630 (W93)
Xilouris K. M., Kramer M., 1996, in Johnston S., Walker M. A., Bailes M., eds, Proc. IAU Coll. 160, Pulsars: Problems and Progress. Astron. Soc. Pac., San Francisco, p. 245 (XK96)
Xilouris K. M., Rankin J. M., Seiradakis J. H., Sieber W., 1991, A&A, 241, 87 (X91)
Xilouris K. M., Seiradakis J. H., Gil J., Sieber W., Wielebinski R., 1995, A&A, 293, 153 (X95)
Zepka A., Cordes J. M., Wasserman I., 1996, ApJ, 456, 305 (Z96)

APPENDIX A: THE CIRCULAR POLARIZATION DATA BASE

Table A1 summarizes the observed circular polarization and variation of linear position angle in mean pulse profiles for pulsars where significant circular polarization is observed. The first two columns give the pulsar J name and B name (if applicable), respectively. In the third column, the sign of $V = I_{LH} - I_{RH}$ across the profile is indicated. Sign reversals are indicated by $+/-$ or $-/+$ and apparently distinct polarization features are indicated by repeated signs. The fourth column gives the sense of position-angle variation across the profile, with 'inc' meaning increasing position angle (i.e. counterclockwise on the sky) and 'dec' meaning decreasing position angle (PA). In some cases, the variation of

PA is complicated by orthogonal jumps or other reasons. Where possible, we have accounted for this in assigning a sense to the PA variation; uncertain cases are marked with 'xx'. A few pulsars have a change in PA sense within the profile – these are marked with, for example, 'i+d'. The following two columns are respectively the observation frequency in megahertz and the reference code, identified at the end of the Table and in the references. Comments are listed in the final column, where '$V(f)$' means that V is a function of observation frequency, and 'dt' is the time resolution of the profile. For pulsars that have been observed by several authors or at different frequencies, we list each observation on a separate line. Where multiple observations at a similar frequency exist, we only list the one with the best signal-to-noise ratio.

Table A1. A summary of pulsar circular polarization observations.

PSR J	PSR B	V	$\langle |V| \rangle / S$ (%)	$\langle V \rangle / S$ (%)	σ (%)	PA	Freq. (MHz)	Ref.	Comments
0034−0721	0031−07	+				dec	268	R83	drifting subpulses
0133−6957		−+	10	−3	3	dec	661	M98	−/+ at centre of pulse
0134−2937		−	13	−8	3	inc	436	M98	−V over profile
0139+5814	0136+57	+				inc	611	LM88	+V for only comp; $L \sim 100\%$
		+	15	15	3	inc	1720	X91	2 comp seen; +V near centre
0141+6009	0138+59	+ − +				dec	415	LM88	interesting profile
0151−0635	0148−06	− −				inc	611	LM88	−V for double cones
0152−1637	0149−16	+−	12	−2	1	inc	660	Q95	+V, −V for 2 comp; large dt; $V(f)$?
		(+)−	8	−5	2	xx	950	V97	no V or weak? PA not clear
0206−4028	0203−40	−	8	−8	2	xx	660	Q95	good detection just at one point
0211−8159		−				xx	661	M98	−V for only high peak component
0255−5304	0254−53	−	4	−3	1	xx	950	V97	PA not clear, maybe dec
0304+1932	0301+19	+ + +				dec	430	R83	+V for the cones and bridge
		+				dec	430	BR80	from individual pulses
		+ + +	10	10	2	dec	1400	R89	the same as at 430 MHz
		+ + +	12	12	3	dec	1720	Mr81	the same as 430 MHz
		+ + +	15	15	4	dec	2650	Mr81	the same as 430 MHz
0332+5434	0329+54	(+) +/−				dec	1700	B82	both modes +/− V for core; $V(f)$
		−/+	13	10	3	dec	1720	Mr81	−/+ for core
		−/+	15	8	3	dec	2650	Mr81	−/+ for core
		+/−	10	−2	3	xx	10550	X95	abnormal mode; +/− V for last comp
0358+5413	0355+54	+ − +				dec	415	LM88	evolves strongly with frequency
		−+	5	−2	1	dec	1720	X91	−V for 1st comp; weak +V 2nd comp
		+(−+)	11	9	3	dec	2650	Mr81	mode changing
		−−	14	−14	2	dec	10550	X95	−V for 2 comp of both modes
0401−7608	0403−76	−	6	−2	1	dec	1440	Q95	−V over profile
0437−4715		+ − + − −/+ + +	13	8	1	dec	438	N97	complex V
		− − −/+ + +	16	−1	1	dec	661	N97	complex $V(f)$
		− + − + − −/+ −+	11	−5	1	dec	1512	N97	complex V
0452−1759	0450−18	− −/+ −				inc	408	LM88	−/+ for core; −V for cone
0454+5543	0450+55	+−	12	−6	2	dec	1700	X91	V for second half
0459−0210		−	18	−10	3	inc	436	M98	−V for peak component
0525+1115	0523+11	−+				xx	1400	R89	−V, +V for 2 comp
0528+2200	0525+21	−				inc	430	R83	−V for one cone; conal double
		− −	3	−3	0	inc	1404	S84a	−V for both cones; best profile!
		−				inc	1420	LM88	−V for 1st cone
0536−7543	0538−75	−	8	−5	1	dec	436	M98	−V over profile
		−	7	−7	1	dec	600	C91	−V over profile
		−	9	−8	1	dec	660	Q95	−V over profile
		+−	11	−6	1	dec	661	M98	+V for first 1/3 profile; −V for rest
		−	11	−9	2	dec	950	V97	similar at 800 MHz
		−	9	−8	1	dec	1440	Q95	−V over profile
0540−7125		−/+	22	1	8	dec	436	M98	−/+ at centre
0543+2329	0540+23	−				dec	430	BR80	−V over profile (individual pulses)
		−				dec	1400	R89	−V over profile
		−				dec	1720	Mr81	as R89
		−				dec	10550	X95	as R89

Table A1 – *continued*

PSR J	PSR B	V	$\langle|V|\rangle/S$ (%)	$\langle V\rangle/S$ (%)	σ (%)	PA	Freq. (MHz)	Ref.	Comments
0601−0527	0559−05	−+	15	−3	3	inc	1440	Q95	bad s/n; −V, + V for 2 comp
		−+				inc	1700	X91	as Q95
0614+2229	0611+22	+				inc	409	LM88	$L \sim 100\%$
		+				inc	430	RB81	as LM88 at 409 MHz
0629+2415	0626+24	−/+				dec	1400	R89	−/+ for cone?
0630−2834	0628−28	−				dec	611	LM88	−V over profile; high L
		−	7	−7	2	dec	649	Mc78	as LM88, but bad s/n
		−	11	−10	1	dec	950	V97	as LM88
		−	10	−9	2	dec	1612	Ma80	as LM88
0631+1036		++				dec	1418	Z96	+V for cone? $L \sim 100\%$
		++				dec	1665	Z96	as at 1418 MHz
0659+1414	0656+14	(+)−				dec	1400	R89	+V not significant
0738−4042	0736−40	−	6	−5	2	xx	631	Mc78	bad s/n and large dt; PA(f)?
		−	7	−6	1	inc	950	V97	−V stronger and over profile
		−	7	−6	1	inc	1612	Ma80	−V for one comp
0742−2822	0740−28	−	2	−2	1	dec	434	M98	weak −V over profile
		−	10	−8	1	dec	660	M98	stronger −V over profile
		−	6	−4	2	dec	800	V97	as 630 MHz by Mc78 but with bad dt
		−	8	−7	2	dec	950	V97	as 660 MHz of M98 but bad dt
		−				dec	1420	LM88	−V for cone?
		−	8	−7	2	dec	1612	Ma80	as LM88 but with bad s/n
0754+3231	0751+32	−−				inc	1400	R89	−V for two (conal?) comp
0758−1528	0756−15	−−	5	−5	2	inc	1700	X91	weak −V for two comp
0820−1350	0818−13	−	19	−19	4	xx	631	Mc78	bad s/n
		−	15	−15	2	inc	950	V97	strong −V for conal double?
		−	7	−5	1	inc	1440	Q95	−V over profile; bad dt
0826+2637m	0823+26m	+/−				inc	430	RB81	+/− for core
		+/−				inc	1400	R89	+/− for core
		−	1	−1	0	inc	1404	S84a	just weak −V
0826+2637p	0823+26p	+				xx	430	RB81	postcursor
		+				xx	1400	R89	strong +V
0828−3417	0826−34	−+				d+i	408	B85	wide profile; −/+ for last two comp
		+ − +				d+i	610	B85	1st comp is stronger and shows +V
0835−4510	0833−45	−	6	−6	1	dec	631	Mc78	Vela pulsar; no V at lower frequency
		−	9	−9	0	dec	950	V97	as Mc78
		−	14	14	1	dec	1612	Ma80	as Mc78; best data
		−−				dec	2295	KD83	−V for two components
0837+0610	0834+06	−−	10	−10	3	xx	636	Mc78	−V for 2 comps
		+/ − −	12	−9	1	xx	800	S84b	+/− for 1st comp; −V for 2nd comp
		−	9	−7	3	inc	950	V97	−V only for 2nd comp
		− + −	5	−3	0	inc	1404	S84a	−V for comps; +V for bridge
		− + −	8	−7	2	inc	1612	Ma80	−V for two comps
0837−4135	0835−41	+	27	27	2	inc	338	H77	strong +V for only comp
		+	35	35	3	inc	405	H77	strong +V for only comp
		+	20	20	1	inc	631	Mc78	as H77; better s/n; PA not clear
		+	30	30	6	xx	800	V97	PA dec? V very strong
		+	18	17	2	dec	950	V97	PA jump? V weaker
		+	6	4	1	inc	1612	Ma80	very weak +V only
0840−5332	0839−53	+	14	9	1	inc	660	Q95	+V for first half profile
		+	15	10	4	inc	1440	Q95	+V for central part; bad s/n
0846−3533	0844−35	−	19	−16	3	dec	950	V97	PA dec, then flat?
		−	12	−8	2	dec	1440	Q95	−V with bad s/n
0907−5157	0905−51	+(−)	9	7	1	inc	660	Q95	+V for central comp of high L
		+−	8	3	2	inc	953	V97	+ − V for two comp of partial cone?
0908−4913	0906−49	+	10	6	1	dec	660	Q95	weak +V for main (stronger) pulse
0922+0638	0919+06	+	9	7	2	inc	950	V97	+V at strongest comp of profile
		+	9	9	1	inc	1404	S84a	+V at maximum
0934−5249	0932−52	+	8	7	3	dec	661	M98	weak +V over profile; bad s/n
		−	17	−17	3	dec	950	V97	−V over profile; bad dt; V(f)?
0942−5552	0940−55	−	14	−2	4	inc	1612	Ma80	−V over profile; bad s/n
0942−5657	0941−56	+	17	12	3	inc	661	M98	+V over profile
		+	23	16	5	inc	1411	Q95	+V for only comp; bad s/n; bad dt
0944−1354	0942−13	−/+	22	14	2	dec	409	LM88	core? two comp at 1.42 GHz (see S95)

Table A1 – *continued*

PSR J	PSR B	V	$\langle|V|\rangle/S$ (%)	$\langle V\rangle/S$ (%)	σ (%)	PA	Freq. (MHz)	Ref.	Comments
0946+0951	0943+10	+				dec	430	RB81	+V for the only comp
0953+0755m	0950+08m	−				dec	800	S84b	weak −V for second half profile
		−	8	−6	0	dec	950	V97	−V over profile
		−				dec	1400	R89	weak V; V(f)?
		−	6	−6	1	dec	1404	S84a	−V for whole profile
		−	9	−9	1	xx	1612	Ma80	worse s/n than S84a
0953+0755i	0950+08i	−+				dec	1400	R89	bad s/n
0955−5304	0953−52	+	13	11	2	xx	661	M98	+V for strongest central component
1001−5507	0959−54	+/−	4	2	1	inc	654	M98	weak +/, for core, but PA not clear
		+/−	5	2	3	inc	950	V97	as 654 MHz but bad s/n
1034−3224		+/−				xx	436	M98	+/− for strongest of more than 6 comp!
1123−4844		+	18	13	5	dec?	436	M98	+V strong between comps
1136+1551	1133+16	−−	15	−15	2	inc	638	Mc78	−V for 2 comps and bridge!
		−−	8	−5	4	inc	950	V97	bad s/n for −V
		− − −	8	−8	1	inc	1404	S84a	−V is complicated for 1st comp
		−−	10	−10	1	inc	1612	Ma80	as Mc78
1157−6224	1154−62	+	20	17	5	dec	631	Mc78	bad s/n for V
		+	15	12	4	dec	950	V97	+V for second part of profile
1202−5820	1159−58	+	10	9	2	inc	436	M98	+V over profile
1210−5559		−	8	−7	2	xx	436	M98	−V over profile; bad dt
1224−6407	1221−63	+	32	15	7	inc	631	Mc78	bad s/n; strong V
		+	33	26	5	inc	950	V97	strong +V
		+	14	13	4	inc	1560	W93	s/n for V just OK, but large dt
		+	20	20	3	inc	1612	Ma80	V is much weaker
1239+2453	1237+25	++/− −				dec	408	LM88	+/− for core
		+ + +/− −				dec	410	M71	+/− for core; +V for two conal comp
		−/+/−				xx	430	B82	normal mode, but ++0+ for abnormal
mode									
		+ + +/− −	13	4	1	dec	1404	S84a	V for cone and core
		++/− −				dec	1700	B82	same V for both modes
		+/−	13	0	4	xx	2700	Mr81	
1243−6423	1240−64	+	19	18	2	inc	631	Mc78	+V for only comp
		+	9	8	3	inc	800	V97	weaker +V
		−/+	6	3	2	inc	950	V97	weaker −/ + V; PA varies
		−	13	−13	2	inc	1612	Ma80	only −V, stronger
1253−5820		+	15	10	3	inc	436	M98	+V over profile
1302−6350	1259−63	+	13	11	2	dec	1520	MJ95	+V seen from one of 2 comp
		+	18	12	3	dec	4680	MJ95	as at 1520 MHz
1320−5359	1317−53	−	7	−5	7	dec	600	C91	weak −V over profile
1326−5859	1323−58	−+	11	6	2	dec	950	V97	−/+ for core
1328−4357	1325−43	−+	10	5	2	inc	436	M98	−/+ for first two of 3 comp
1328−4921	1325−49	+/−	18	0	6	xx	436	M98	+/− near centre
1338−6204	1334−61	+	10	6	2	i+d	1440	Q95	weak +V in central part
1341−6220	1338−62	−	25	−12	9	inc	1411	Q95	bad s/n for −V; L~90%
1357−6228	1353−62	−	16	12	5	dec	1612	Ma80	bad s/n for −V over profile
1359−6038	1356−60	+	22	22	2	inc	660	M98	+V over profile; L~ 100%
		+−	15	4	4	inc	1560	W93	bad s/n for −V and bad dt
1453−6413	1449−64	++	11	9	1	inc	400	H77	+V varies with frequency?
		++	6	5	2	inc	950	V97	3 components?
1456−6843	1451−68	−/+	8	4	1	dec	400	H77	−/+ for core; same at 271 MHz (R83)
		− −/++	6	0	1	dec	649	Mc78	as at 400 MHz; −/+ at centre
		− −/++	6	3	0	dec	950	V97	two comp in core
		− −/++	7	−1	1	dec	1612	Ma80	symmetric V?
1509+5531	1508+55	+/−				dec	610	LM88	+/− over triple profile
		++/− −	8	0	2	dec	1612	Mr81	as 610 MHz
1527−3931	1524−39	+	18	8	6	dec	436	M98	+V for conal double; bad s/n
		+	20	13	5	dec	661	M98	as at 436 MHz
1527−5552	1523−55	−/+	20	13	2	dec	661	M98	−/+ for the core?
1534−5334	1530−53	+/−				dec	960	V97	+/− for the first strong comp
		+/−	8	−4	2	dec	1612	Ma80	as V97, partial cone?
1537+1155	1534+12	− −/+				dec	430	A96	+/− for main comp
1542−5304		+	16	10	5	inc	661	M98	+V in 2nd half of profile

Table A1 – *continued*

PSR J	PSR B	V	⟨|V|⟩/S (%)	⟨V⟩/S (%)	σ (%)	PA	Freq. (MHz)	Ref.	Comments
1543+0929	1541+09	+ − +				d+i	430	R83	possible 7 comp; strong −V at centre
		+ − +	13	−1	2	d+i	1400	R89	V seen over the very wide profile
1544−5308	1541−52	− − / + +	11	1	2	xx	661	M98	−/+ for central comp
1557−4258		−	13	−8	2	dec	661	M98	−V for central comp with strong L
1559−4438	1556−44	−	12	−12	2	dec	631	Mc78	L ∼ 60%
		−+	5	3	1	dec	661	M98	V variable?
		−	8	−7	4	dec	800	V97	weaker V
		−	13	−10	3	dec	950	V97	−V stronger
		−/+	11	−8	1	dec	1490	M98	resolved profile with interesting V
		−	8	−4	3	dec	1560	W93	weak −V
		−	16	−15	2	dec	1612	Ma80	−V at centre
1600−5044	1557−50	+	21	20	5	inc	950	V97	bad s/n, scattering
		+	16	14	2	inc	1560	W93	bad dt; +V in part of profile
		+	23	21	4	inc	1612	Ma80	as W93
1604−4909		+/−	6	3	1	inc	661	M98	+/− for core
1607−0032	1604−00	−/++				dec	430	R88	−/+ for one comp; +V for another comp
		−	9	−7	2	xx	631	Mc78	−V over most of profile
		+ − +				xx	1400	R89	+V doubtful; −V OK
1614−5047	1610−50	+	26	10	12	dec	1411	Q95	bad dt
1633−5015	1629−50	−	18	−13	3	inc	1411	Q95	strong −V over profile
1635+2418	1633+24	−(+)				dec	1400	R89	−V for central comp
1644−4559	1641−45	−	3	−2	0	inc	950	V97	weak −V over scattered profile
		(−) + −	4	−1	1	inc	1612	Ma80	+V for peak
1646−6831	1641−68	+(−)	12	5	1	i+d	660	Q95	+V at centre
		+(−)	14	5	3	i+d	953	V97	bad s/n for −V; PA = inc+dec?
1645−0317	1642−03	+/−				xx	408	LM88	complicated PA
		−				xx	410	M71	−V over profile
		−	8	−7	1	inc	631	Mc78	−V for the only comp; V(f)?
		−	3	−2	1	dec	950	V97	−V for the only comp; PA(f)?
1651−4246	1648−42	−	19	−13	4	dec	950	V97	−V for 2nd part of profile; bad s/n
		−	11	−3	4	dec	1560	W93	as at 950 MHz; better s/n
1700−3312		−	27	−24	8	inc	434	M98	−V over profile, but with bad s/n
1703−3241	1700−32	−/+	7	−1	2	inc	950	V97	−/+ for core
		−/+	10	−2	3	inc	1612	Ma80	−/+ for core seen at 409 MHz (LM88)
1705−1906m	1702−19m	−	60	−60	3	dec	408	B88	large −V over whole profile
1705−1906i	1702−19i	−	60	−60	3	dec	408	B88	also large −V
1709−4428	1706−44	−	17	−16	3	inc	1440	Q95	−V over only comp; L up to 90%
1713+0747		−/+				i+d	1400	XK96	−/+ for core? PA inc+dec?
1721−3532	1718−35	−	17	−14	4	dec	1411	Q95	−V appears at strongest part of profile
1722−3712	1719−37	+	9	8	2	inc	661	M98	weak +V over profile; high L
1731−4744	1727−47	+	9	7	3	xx	400	H77	bad s/n and PA not clear
		+	5	4	1	dec	800	V97	weak +V for 1st comp; same at 950 MHz
1740−3015	1737−30	−	20	−19	2	dec	660	Q95	−V over profile; bad dt and bad s/n
		−	22	−22	3	dec	1560	W93	−V strong at 2nd half of only comp
1740+1311	1737+13	+ + /−				dec	430	R88	+/− for core and +V for cone
		+ + + /−				dec	1400	R89	as R88
1741−3927	1737−39	+	7	4	1	xx	661	M98	weak +V over profile
		+	10	7	3	inc	954	V97	+V at centre; bad dt
1745−3040	1742−30	−	10	−9	3	xx	950	V97	PA and V similar to X91
		− − −	15	−15	2	xx	1700	X91	−V for 3 (conal?) comp
1751−4657	1747−46	−/++	12	8	1	dec	436	M98	−/+ for 1st comp; 2nd comp +V
		+	8	6	1	dec	631	Mc78	+V at centre
		−/++				dec	950	V97	as M98 at 1522 MHz
		−/++	9	6	2	dec	1522	M98	same as 436 MHz
1752−2806	1749−28	−	7	−7	1	xx	631	Mc78	bad dt; V(f)?
		−	3	−2	0	dec	950	V97	V(f), PA(f)
		−(/+)	5	1	1	xx	1612	Ma80	weak +V; bad dt
		−/+	5	0	3	xx	1720	Mr81	−/+ for core?
		−/+	13	11	3	dec	2650	Mr81	−/+ for core? 3 comp?
1801−0357		+/−	20	−6	4	dec	661	M98	+/− for core, but PA not clear
1803−2137	1800−21	++	21	20	3	dec	1560	W93	interesting profile with high L
1807−0847	1804−08	+ − −	10	0	2	xx	1700	X91	very weak V for central and last comp
1817−3618	1813−36	−	13	−10	1	xx	660	Q95	strong −V over part profile; bad dt

Table A1 – *continued*

PSR J	PSR B	V	⟨|V|⟩/S (%)	⟨V⟩/S (%)	σ (%)	PA	Freq. (MHz)	Ref.	Comments
1820−0427	1818−04	−				xx	410	M71	−V over part profile
		−	18	−12	4	inc	631	Mc78	poor s/n
		−	13	−6	3	inc	950	V97	better s/n
1823+0550	1821+05	+ + / − −	11	2	2	dec	1400	R89	+/− for core; PA not clear
1829−1751	1826−17	−	19	−17	2	xx	436	M98	strong −V; scattered profile; flat PA
		−	15	−11	2	d+i	660	M98	strong −V over profile; PA= dec+inc!
		−	17	−11	5	xx	950	V97	PA inc+dec?
1836−1008	1834−10	−+	10	−3	3	dec	1720	X91	weak −/+ at pulse centre; poor s/n
1841+0912	1839+09	+ − +	5	−3	1	dec	1400	R89	+ − + for 3 comp; +V very weak
1848−1952	1845−19	−	14	−13	5	xx	950	V97	−V for 1st resolved component
1852−2610		+	9	2	3	dec	436	M98	strong L, weak V
1857+0943	1855+09m	+−				dec	1400	S86	+−V for 2 comp
1900−2600	1857−26	+/−				xx	170	R83	+/− for core comp
		+/ − −				xx	268	R83	+/− for core comp
		+ + / − −	17	−3	4	dec	631	Mc78	+/− for central part
		+/−	12	2	2	dec	661	M98	+/− for central part
		+/−	12	−1	1	dec	950	V97	+/− for central part
		+/−	16	−2	1	dec	1490	M98	+/− for central part
		+ + / − −	20	−1	3	dec	1612	Ma80	+/− over most of profile
		+/−	22	0	4	dec	2650	Mr81	
1901+0331	1859+03	+/−	12	3	2	dec	1400	R89	+/− for core
1903+0135	1900+01	+	13	8	4	inc	950	V97	+V for central comp only
1907+4002	1905+39	− −	10	−10	3	dec	1700	X91	−V for 2 comp; s/n just OK
1909+0254	1907+02	−/+				dec	430	RB81	triple at 1410 MHz (S95)
1910+0358	1907+03	(−+)−	16	−13	2	dec	1400	R89	strong −V from 2nd half profile
1909+1102	1907+10	−	12	−12	2	inc	1400	R89	−V for core only?
1910+1231	1908+12	+				xx	430	RB81	s/n for +V just OK
1912+2104	1910+20	−				inc	1400	R89	s/n for −V just OK
1913−0440	1911−04	+ − +	15	−1	4	xx	400	H77	bad s/n for V
		+−	8	−5	2	inc	950	V97	+− for two unresolved comp?
1913+1400	1911+13	+ − (+)				xx	1400	R89	bad s/n for +V; PA=dec?
1915+1009	1913+10	+	40	40	2	d+i	1400	R89	very strong +V over profile
1915+1606	1913+16	−/+ +−				inc	430	C90	−/+ for 1st comp
1915+1647	1913+167	+				dec	430	RB81	+V at centre
		+/−				xx	1400	R89	two core comps
1916+0951	1914+09	−				dec	430	RB81	−V for 1st comp
		+				dec	1400	R89	weak +V over profile
1916+1312	1914+13	−	37	−37	2	inc	1400	R89	very strong −V over profile
1917+1353	1915+13	−				dec	430	RB81	−V for only comp
		−				dec	1400	R89	−V over profile
1918+1444	1916+14	+				xx	430	RB81	bad s/n
		+				dec	1400	R89	+V over profile
1919+0021	1917+00	+				xx	418	RB81	+V for core
		+ + −				inc	1400	R89	triple profile, +/−?
1921+1419	1919+14	+−				dec	430	RB81	+V weak, −V strong
		+−				dec	1400	R89	−V not so strong
1922+2110	1920+21	+	20	3	2	dec	430	RB81	+V for core? bad dt
1926+1648	1924+16	−/+				inc	430	RB81	−/+? high L
		+				inc	1400	R89	weak +V over profile
1932+1059m	1929+10m	− −				dec	430	BR80	−V for all comps; L ∼ 100%
		+ + − −	2	0	0	dec	800	S84b	V very weak; +/ − V for central comp
		− −				dec	1400	R89	weaker −V for 2 or 3 comp
		− −	1	−1	0	dec	1404	S84a	weaker −V for 3 comp
		− −				dec	1665	P90	−V for all at 1665 and 430 MHz
		++				dec	1700	X91	very weak +V for all
1932+1059i	1929+10i	−				inc	430	RB81	−V for main comp
		−				xx	1400	R89	−V for core?
		−				inc	1665	P90	−V for all at 430 and 1665 MHz
1932−3655		+/−	22	9	8	inc	658	M98	significant +/ − V for the peak comp
1935+1616	1933+16	−/+				xx	430	R83	−/+ for core
		−/+	15	−1	1	xx	1440	R89	−/+ for two core comps
		−/+	14	0	3	xx	1720	Mr81	good s/n
		−/+	15	0	3	xx	2700	Mr81	−/+ for core

Table A1 – *continued*

PSR J	PSR B	V	$\langle|V|\rangle/S$ (%)	$\langle V\rangle/S$ (%)	σ (%)	PA	Freq. (MHz)	Ref.	Comments
1939+2134m	1937+21m	−				xx	1418	TS90	across whole pulse
1939+2134i	1937+21i	−				xx	1418	TS90	
1941−2602	1937−26	−	13	−7	5	dec	1560	W93	weak −V; s/n just OK
1946+1805	1944+17	−(+) − −	5	4	1	inc	1404	S84a	V over profile
1946+2244	1944+22	−				xx	430	RB81	s/n just OK
1946−2913	1943−29	+	15	9	6	inc	434	M98	+V just for central strong comp
1948+3540	1946+35	+				xx	430	RB81	+V for scattered profile
		++				inc	1400	R89	+V for 2 or 3 comp
1954+2923	1952+29	− − +−				inc	430	RB81	strong −V
		− − − + −	21	−19	2	dec?	1400	R89	−V over most of profile
1959+2048m	1957+20m	(+)/−				xx	430	TS90	MSP; very weak L
		−/+				xx	430	F90	V appears to be reversed to TS90
1959+2048i	1957+20i	+−				xx	430	TS90	as main pulse
		−+				xx	430	F90	as main pulse
2004+3137	2002+31	+/−				xx	430	RB81	+/− for core; bad dt
		+/−	4	0	1	inc	1400	R89	PA is not so clear
2006−0807	2003−08	− +/ − −	14	−11	2	inc	1700	X91	+/− core; −V for cone
2018+2839	2016+28	−	6	−6	1	inc	1404	S84a	−V for central part
2022+2854	2020+28	+/ − −−				inc	430	C78	but also show −− for two cones!
		+/ − −−	8	−7	0	inc	800	S84b	+/− for 1st comp
		+/ − −−	7	−7	0	inc	1404	S84a	as at 800 MHz, but +/− weak
2022+5154	2021+51	−	4	−4	1	inc	10550	X95	weak −V
2021+2145	2025+21	+				dec	430	RB81	s/n just OK
2030+2228	2028+22	++				dec	1400	R89	weak +V for 2 comps
2046−0421	2043−04	−				xx	950	V97	−V for strongest comp
2046+1540	2044+15	+ + +				i+d	1400	R89	very weak +V for 2 comp
2048−1616	2045−16	+ − +	7	3	1	dec	950	V97	+V for outer conal comps
		++/ − +				dec	1420	LM88	weak +/− for core; +V for conal comps
2053−7200	2048−72	+−	13	−4	1	inc	660	Q95	+ − V for 2 comp with bad s/n
		+/−	8	−2	2	inc	661	M98	confirm + − V seen by Q95
		+−				inc	950	V97	+− V for two comps
		−+	10	−5	2	inc	1440	Q95	bad s/n for V; $V(f)$?
2055+3630	2053+36	−				xx	1400	R89	bad s/n
2113+2754	2110+27	−−				dec	1400	R89	weak V
2113+4644	2111+46	+/−				dec	610	LM88	+/− for core
		+/−	10	0	3	dec	1720	Mr81	also 2650 MHz
2116+1414	2113+14	+/−				inc	1400	R89	+/− at centre but not peak
2144−3933		−/+	17	3	2	inc	661	M98	−/+ for core
2145−0750		−+				inc?	1400	XK96	PA variation not clear
2155−3118	2152−31	+	25	22	7	dec?	950	V97	strong +V, weak L
2219+4754	2217+47	+				inc	1612	Mr81	but at 2650 MHz, weak −V?
2225+6535	2224+65	−−				dec	408	LM88	−V for 2 comps; bad s/n; PA=dec+flat
2305+3100	2303+30	++				inc	1400	R89	weak +V over comp; good s/n
2313+4253	2310+42	− + −	13	−11	1	inc	1700	X91	V over profile
2317+2149	2315+21	−				inc	409	LM88	core? bad dt; bad s/n
		− − −				xx	1400	R89	−V varies for 2 (or 3) comp
2324−6054	2321−61	+	13	11	1	dec	660	Q95	+V for 1 of 2 (conal) comp
		+(−)				dec	950	V97	bad s/n for V
2330−2005	2327−20	−−	22	−22	1	inc	648	Mc78	strong −V over whole profile
		−−	12	−11	1	inc	950	V97	weaker −V; good s/n
2346−0609		+	11	9	2	dec	436	M98	conal double; +V for second comp
2354+6155	2351+61	++	9	9	3	dec	1700	X91	+V for two comp

Notes to table.

References: Manchester 1971 (M71); Hamilton et al. 1977 (H77); Cordes, Rankin & Backer 1978 (C78); McCulloch et al. 1978 (Mc78); Backer & Rankin 1980 (BR80); Manchester, Hamilton & McCulloch 1980 (Ma80); Morris et al. 1981 (Mr81); Rankin & Benson 1981 (RB81); Barter et al. 1982 (B82); Krishnamohan & Downs 1983 (KD83); Rankin 1983 (R83); Stinebring et al. 1984a (S84a); Stinebring et al. 1984b (S84b); Biggs et al. 1985 (B85); Segelstein et al. 1986 (S86); Biggs et al. 1988 (B88); Lyne & Manchester 1988 (LM88); Rankin, Wolszczan & Stinebring 1988 (R88); Rankin, Stinebring & Weisberg 1989 (R89); Cordes, Wasserman & Blaskiewicz 1990 (C90); Fruchter et al. 1990 (F90); Phillips 1990 (P90); Thorsett & Stinebring 1990 (TS90); Costa et al. 1991 (C91); Xilouris et al. 1991 (X91); Wu et al. 1993 (W93); Gould 1994 (G94); Manchester & Johnston 1995 (MJ95); Qiao et al. 1995 (Q95); Seiradakis et al. 1995 (S95); Xilouris et al. 1995 (X95); Arzoumanian et al. 1996 (A96); Xilouris & Kramer 1996 (XK96); Zepka, Cordes & Wasserman 1996 (Z96); Navarro et al. 1997 (N97); van Ommen et al. 1997 (V97); Manchester, Han & Qiao 1998 (M98).

'm' or 'i' following the pulsar name refer to main pulse or interpulse, respectively.

This paper has been typeset from a T_EX/L^AT_EX file prepared by the author.